 Erosion and Sediment Yields in the Changing Environment (Proceedings of a symposium held at the Institute of Mountain Hazards and Environment, CAS-Chengdu, China, 11–15 October 2012) (IAHS Publ. 356, 2012).

MODIS-based remote sensing of suspended sediment concentrations of the Middle and Lower Yangtze River, China

XI-XI LU[1], JIAN-JUN WANG[2] & CHENG LIU[3]

1 Department of Geography, National University of Singapore; 10 Kent Ridge Crescent, 119260, Singapore

2 Department of Geodesy and Geomatics Engineering, University of New Brunswick; 15 Dineen Drive, PO Box 4400, Fredericton, New Brunswick E3B 5A3, Canada
t6jxc@unb.ca

3 International Research and Training Center on Erosion and Sedimentation (IRTCES); IRTCES, PO Box 366, No. 20 Chegongzhuang Road West, Beijing, 100048, China

Abstract Suspended sediment concentration (SSC) is a critical parameter in the study of river sediment transport and water quality variations. The potential for estimating SSC in large rivers using satellite images has been examined in previous studies. Using the Middle and Lower Yangtze River as an example, this paper applies a simple segmented linear regression to eliminate the errors of SSC estimation caused by the nonlinear relation between spectral reflectance and the SSC of turbid rivers. In comparison to previous studies, this one improves the accuracy of estimated SSC values based on the high temporal resolution Terra Moderate Resolution Imaging Spectroradiometer (MODIS) images. The improvement was particularly significant for water samples with high SSC values. This is crucial for studying the spatial and temporal variations of SSC in large rivers that can result from climate change and human activities such as dam construction and illegal sand extractions.

Key words satellite remote sensing; suspended sediment concentration (SSC); Terra MODIS images; turbid water; Yangtze River

INTRODUCTION

Human activities such as the construction of large numbers of reservoirs have changed the sediment regime of the Yangtze River during recent decades. Based on the sediment records at four hydrologic stations on the Yangtze River, Li *et al*. (2011) concluded that the impacts on the sediment regime varied with reservoir storage capacity, operational modes, and the distance between the target reservoir and the specific site. Such changes may cause further impacts on the health and stability of the Yangtze River ecosystem.

In particular, since the filling of the reservoir behind the Three Gorges Dam in 2003, the reach between the dam and the Hankou station (Fig. 1) has become a significant sediment source rather than a sediment sink, according to the records at the two hydrologic stations at Yichang and Hankou (Yang *et al*., 2011). Nevertheless, Dai *et al*. (2011) argued that climate effects could not be ignored. For example, their analysis of a time series of water and sediment records suggested that the historical low values for sediment discharge into the Yangtze estuary in 2006 were mainly attributable to extreme drought conditions, rather than the Three Gorges Dam.

In order to assess the impacts of human activities and climate on sediment deposition and transport in the Yangtze River, records of suspended sediment concentration (SSC) are required. Moreover, SSC data also are required when evaluating potential ecological risk due to sediment-associated heavy metal contamination. For instance, Ma *et al.* (2011) found that in Yangtze River sediments collected adjacent to the downtown section of Chongqing, the concentrations of heavy metals were Zn > Cu > Pb > As > Cd > Hg. Hence, SSC is also crucial to the investigation of heavy metal sources (e.g. are they from upstream sources or locally derived?).

However, spatially and temporally continuous sediment records are scarce for most rivers in the world (Syvitski *et al*., 2000). For example, there are only five main hydrologic stations, with relatively temporally continuous sediment records, on the Yangtze mainstream from Jianli downstream to the river mouth. The severe lack of sediment records may be attributed to the high cost, and time-consuming methods currently associated with collecting *in situ* measurements (Gao & O'Leary, 1997), as well as poor transportation conditions, etc.

As a result of their wide spatial coverage and high temporal repeatability, remote sensing techniques have been used to estimate SSC values directly from satellite data. Most previous

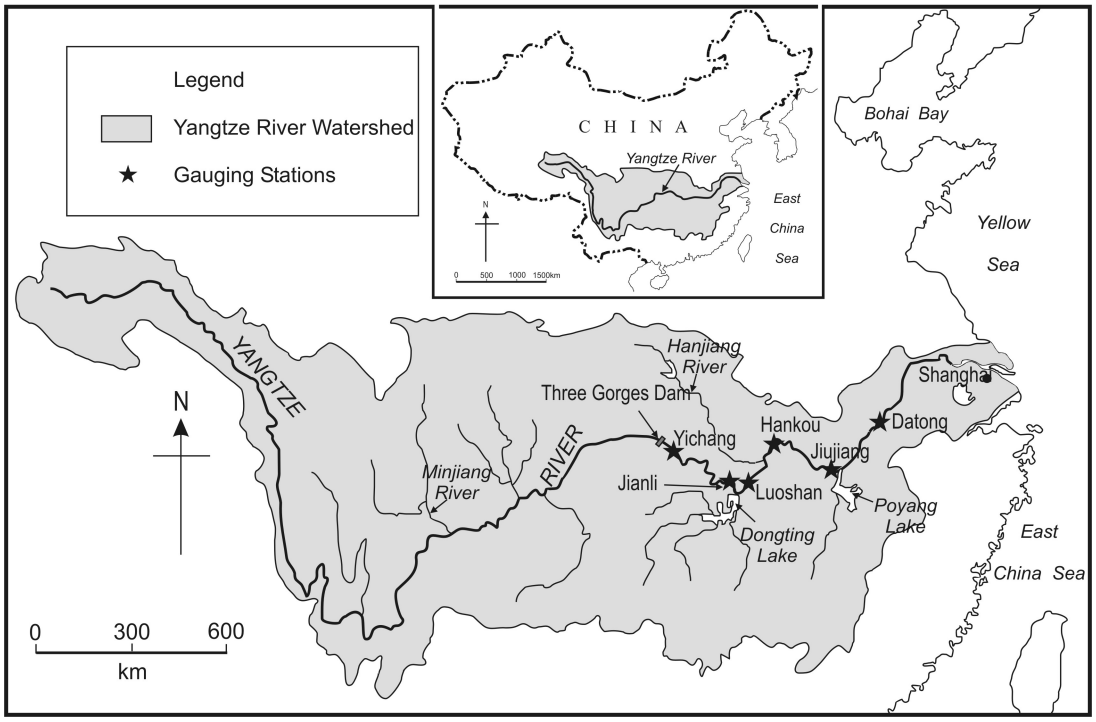

Fig. 1 Map of the Yangtze River basin showing the locations of gauging stations used in this study. In total, 153 samples at five stations, *i.e.* Jianli (29), Luoshan (31), Hankou (25), Jiujiang (35) and Datong (33) downstream, were employed in this study.

studies have focused on coastal waters, estuaries and lakes (e.g. Dekker *et al*., 2002; Doxaran *et al.*, 2002; Ouillon *et al*., 2004; Milier & Mckee, 2004; Ma & Dai, 2005; Zhou *et al*., 2006). However, more recently, river waters are attracting more and more attention (e.g. Islam *et al*., 2001; Onderka & Pekarova, 2008; Wang *et al*., 2009, 2010).

The potential for estimating the SSC in large rivers was examined in previous studies on the Amazon River (e.g. Martinez *et al*., 2007) and on the Yangtze River (Wang *et al*., 2010). Wang *et al.* (2010) employed high temporal resolution Terra Moderate Resolution Imaging Spectro-radiometer (MODIS) data because its high resolution (1–2 days) is necessary for the accurate monitoring of dynamic changes in river systems. They found that the water reflectance difference between Bands 2 and 5, denoted as $\rho_{,w,2} - \rho_{,w,5}$, in conjunction with a linear regression model, could be used to produce relatively accurate SSC estimates.

Although, SSC showed a strong linear regression relation with $\rho_{,w,2} - \rho_{,w,5}$ within the range of 74–881 mg L^{-1}, it was clear that the relationship became nonlinear when concentrations exceeded 600 mg L^{-1} (Wang *et al.*, 2010). As a result, all the samples with SSCs in the range of 600–881 mg L^{-1} were underestimated. Therefore, the current study, focused on the nonlinear relation between SSC and reflectance within a wide SSC range (i.e. 74–881 mg L^{-1}), to develop a more precise regression model that was suitable for use throughout the Middle and Lower Yangtze River reaches.

STUDY AREA

The 6300 km-long Yangtze River is the third longest river in the world (Fig. 1; Yangtze River Water Resources Committee, 2006). The Middle and Lower Yangtze River refers to the downstream reach from Yichang City, which is near the Three Gorges Dam (TGD), the largest dam in the world (Nilsson *et al*., 2005). During recent decades, the Yangtze River Basin has undergone dramatic environmental changes due to extensive human activities such as reservoir construction. As a result, obvious changes in soil erosion and sediment yields have been observed

(Lu & Higgitt, 1998; Yang *et al*., 2005; Long *et al*., 2006). In particular, more than 50 000 dams of different sizes have been built throughout the Yangtze River Basin to store water, minimize flooding, and generate electricity (Yang *et al*., 2005, 2011).

DATA AND METHODS

As this study was designed to develop a more quantitative relationship between SSC and reflectance based on the Wang *et al.* (2010) study in the Middle and Lower Yangtze River, the same SSC and Terra MODIS data also were used in this study. In addition, their image processing methods and procedure were also applied herein.

In total, there are five hydrologic gauging stations with sediment records along the Middle and Lower Yangtze River from Jianli to Datong (Fig. 1). These five gauging stations upstream to downstream, are Jianli, Luoshan, Hankou, Jiujiang and Datong. They are national-level stations where routine water and sediment measurements are produced using nationally standardized methods (Ministry of Water Resources of China, 1992). In general, the daily SSC data collected at each station are generated from point-integrated samples collected at 0.2, 0.6 and 0.8% of water depth at ten cross-sectional verticals.

The current study involved the SSC data collected at those five stations during the 2005 wet season (May–October). The Terra MODIS L1B images acquired on the corresponding dates were downloaded from the MODIS Data Service Center website, Institute of Industrial Science, University of Tokyo, Japan (http://webmodis.iis.utokyo.ac.jp/). Cloudy days were excluded. In total, this study used 153 samples with SSCs ranging from 74 to 881 mg L^{-1} that had been collected at the five stations; each station generated 25–35 samples.

From the Terra MODIS images, a pixel of river water was chosen based on its geographic location, Band 2 radiance, and band combination RGB = 765 (Wang *et al*., 2010). As the downloaded MODIS images include data on the top-of-atmosphere (TOA) pixel radiance, the TOA reflectance was calculated directly. To convert the TOA reflectance into water reflectance, atmospheric corrections were applied following the detailed procedures described in Wang *et al*. (2009). Fortunately, this atmospheric correction method does not require data on *in situ* atmospheric conditions that often are unavailable.

In previous remote sensing studies applied to aquatic systems, regression analyses were widely applied to develop an SSC–water reflectance relation. This study divided all 153 samples into two groups because SSC showed a strong linear relation with reflectance values in each of the groups. Then, separate linear regression analyses were conducted within each group.

To assess the accuracy of the SSC values generated from the reflectance data, several factors including: absolute relative error (ARE in %), root mean square error (RMSE in mg L^{-1}), and relative root mean square error (RRMSE in %) were calculated as follows:

$$ARE = \left| \frac{SSC - SSC'}{SSC} \times 100\% \right| \tag{1}$$

$$RMSE = \sqrt{\frac{\sum_{i=1}^{n} \left(SSC_i - SSC_i'\right)^2}{n}} \tag{2}$$

$$RRMSE = RMSE \Big/ \left(\frac{\sum_{i=1}^{n} SSC_i}{n} \right) \times 100\% \tag{3}$$

where SSC_i refers to observed SSC, SSC_i' is estimated SSC, and n refers to the number of samples.

The SSC–reflectance regressions were then applied to Terra MODIS images that were not used to generate the final SSC–reflectance models.

RESULTS

SSC-water reflectance relations

Wang *et al.* (2010) used a single linear regression model to describe the relation between $\rho_{,w,2} - \rho_{,w,5}$ and SSC for all samples. However, it can be seen from Fig. 2(a) that although the reflectance differences of $\rho_{,w,2} - \rho_{,w,5}$ increase with SSC, such increases become smaller with increasing SSC. As shown in Fig. 2(a), SSC shows different linear relations with $\rho_{,w,2} - \rho_{,w,5}$ if we use $\rho_{,w,2} - \rho_{,w,5}$ = 8% as a breakpoint to cluster all the 153 samples into two groups.

Thus, the relation between SSC and $\rho_{,w,2} - \rho_{,w,5}$ was fitted:

$$Y = 50.15X + 17.76 \qquad \text{for } \rho_{,w,2} - \rho_{,w,5} < 8\% \tag{4}$$

(Y = SSC in mg L^{-1}, $X = \rho_{,w,2} - \rho_{,w,5}$ in percentage, $R^2 = 0.60$, $n = 137$, $p < 0.001$)

$$Y = 112.77X - 485.49 \qquad \text{for } \rho_{,w,2} - \rho_{,w,5} \geq 8\% \tag{5}$$

(Y = SSC in mg L^{-1}, $X = \rho_{,w,2} - \rho_{,w,5}$ in percentage, $R^2 = 0.45$, $n = 16$, $p < 0.005$).

In general, the residuals were distributed in the region of ±175 mg L^{-1} for each group (Fig. 2(b)). For all 153 samples, the mean ARE was 23.3%, the RMSE was 76 mg L^{-1}, and the RRMSE was 27.5% (Table 1). For the first group ($\rho_{,w,2} - \rho_{,w,5} < 8\%$), the mean ARE was 23.8%, the RMSE was 66 mg L^{-1}, and the RRMSE 27.4%. For the second group ($\rho_{,w,2} - \rho_{,w,5} \geq 8\%$), the mean ARE was 18.7%, the RMSE was 133 mg L^{-1}, and the RRMSE was 23.0%. Both the mean ARE and RRMSE are smaller for the second group than for the first group. Hence, the estimations for the samples with higher SSC values are more accurate as $\rho_{,w,2} - \rho_{,w,5}$ and SSC have positive relations. The observed and the estimated SSC values were compared in Fig. 3(a). The data points were distributed along and close to the 1:1 line.

Table 1 Comparison of SSC valued estimated in this study and Wang *et al.* (2010), respectively.

Samples	Sample no.	Mean SSC (mg L^{-1})	This study Mean ARE (%)	RMSE (mg L^{-1})	RMSE (%)	Wang *et al.* (2010) Mean ARE (%)	RMSE (mg L^{-1})	RMSE (%)
$\rho_{,w,2} - \rho_{,w,5} < 5\%$	137	240	23.8	66	27.4	25.8	68	28.6
$\rho_{,w,2} - \rho_{,w,5} \geq 8\%$	16	578	18.7	133	23.0	21.0	154	26.6
All samples	153	275	23.3	76	27.5	25.3	81	29.7

Application of the regression relation

A Terra MODIS image acquired on 10 September 2005 was employed to estimate SSC values using the two regression equations (4) and (5) developed during this study. From Jianli to Datong, 20 sites with similar spatial intervals were chosen, including five hydrologic gauging stations with sediment records (i.e. Jianli, Luoshan, Hankou, Jiujiang and Datong). The estimated SSC values are shown in Fig. 4. The ARE values are 2.6%, 2.8%, 1.5%, 0.8% and 3.9% at these five stations, respectively, and the mean ARE is 2.3%. Hence, the estimated SSC values were quite similar to the observed ones at the five stations.

DISCUSSION

Relation of SSC–reflectance difference between Bands 2 and 5

When all 153 data points were fitted using a single linear regression, as done in Wang *et al.* (2010), the mean ARE was 25.3% with an RMSE of 81 mg L^{-1}, and an RRMSE of 29.7% (Table 1). For the samples whose $\rho_{,w,2} - \rho_{,w,5}$ values were < 8%, the mean ARE was 25.8%, with an RMSE 68 mg L^{-1}, and an RRMSE 28.6%. For the samples with $\rho_{,w,2} - \rho_{,w,5}$ values ≥ 8%, the mean ARE was 21.0%, with an RMSE of 154 mg L^{-1}, and an RRMSE of 26.6%. In comparison to Wang *et al*. (2010), this study generated more accurate estimations for each group with both lower or higher SSC values, or with smaller or greater $\rho_{,w,2} - \rho_{,w,5}$ values.

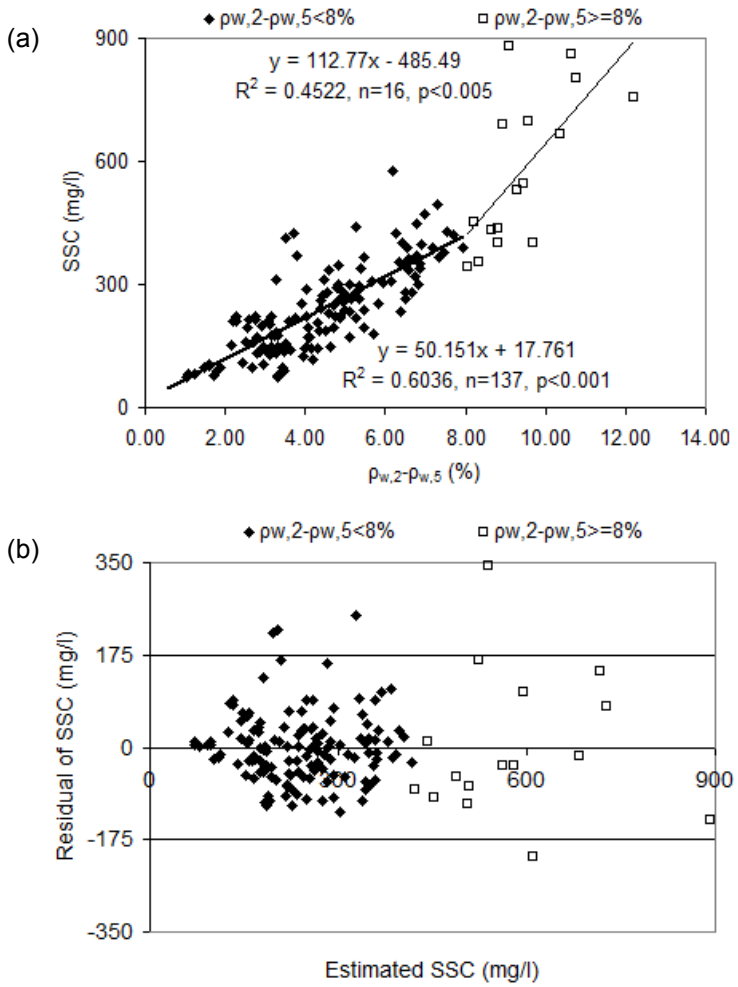

Fig. 2 (a) Relation of observed SSC and the water reflectance difference between Bands 2 and 5 (denoted as $\rho_{,w,2} - \rho_{,w,5}$). (b) Residual of SSC *vs* estimated SSC. Note that a simple segmented linear regression was used in this study.

Wang *et al.* (2010) used a single linear regression model to represent the relation between SSC and $\rho_{,w,2} - \rho_{,w,5}$ for all samples, but it appears that the linear relation changed when $\rho_{,w,2} - \rho_{,w,5} \geq 8\%$, as shown in Fig. 2(a). This led to a systematic error: samples were underestimated in the SSC range of 600–900 mg L^{-1}. In contrast, this study used two linear regression models to describe the relation of SSC and $\rho_{,w,2} - \rho_{,w,5}$. In comparison to Wang *et al.* (2010), it can be seen clearly from Fig. 3 that fewer samples were overestimated for the SSC range of 300–400 mg L^{-1}, and fewer samples were underestimated for the SSC range of 600–900 mg L^{-1} in this study.

A number of studies (e.g. Lathrop & Lillesand, 1989; Stumpf & Pennock, 1989; Han & Rundquist, 1994; Bowers *et al.*, 1998) have indicated such saturation behaviour (i.e. reflectance increases with increasing water quality parameters); however, increasing reflectance becomes less and less significant. The saturation may appear at higher reflectances at longer wavelengths (Harrington *et al.*, 1992; Doxaran *et al.*, 2002; Wang *et al.*, 2009). A single linear relationship does not appear to be suitable for both low and high concentrations (Bowers *et al.*, 1998). Hence, this may explain why the current study significantly reduced the SSC estimation errors at both low and high SSCs because two linear regressions were used rather one.

Application of the regression relation

To demonstrate how their empirical relation would behave, Wang *et al.* (2010) estimated SSC at 20 selected sites along reaches of the Middle and Lower Yangtze River between Jianli and Datong

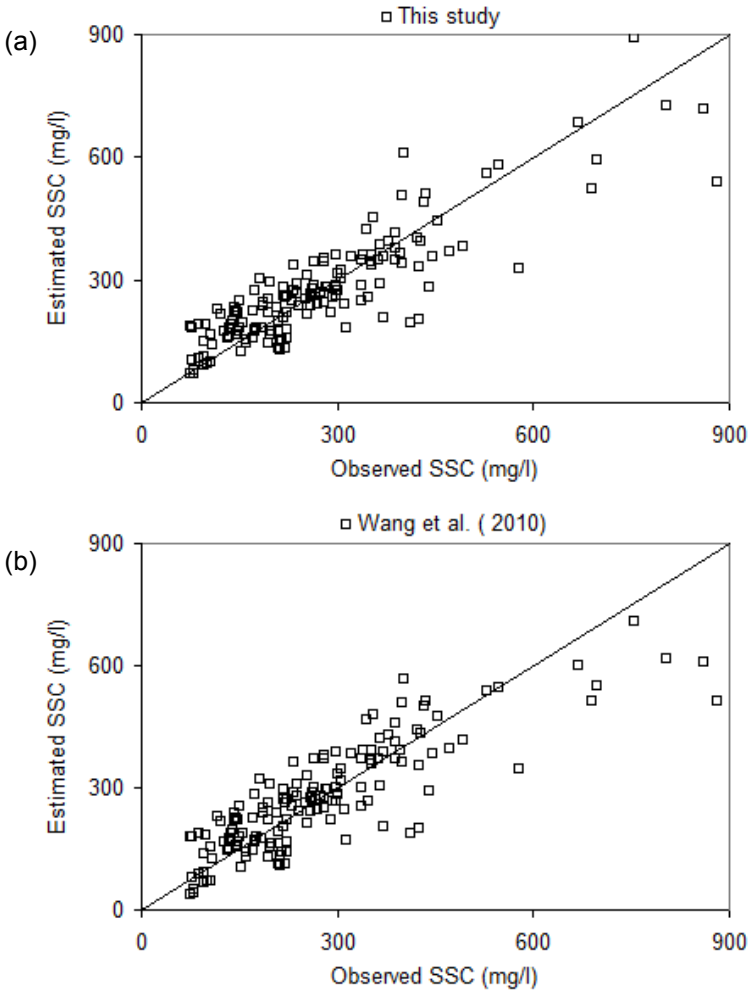

Fig. 3 Scatter plots of observed SSC against estimated SSC of the Middle and Lower Yangtze River, where the line indicates a 1:1 relationship: (a) this study; (b) Wang *et al*. (2010).

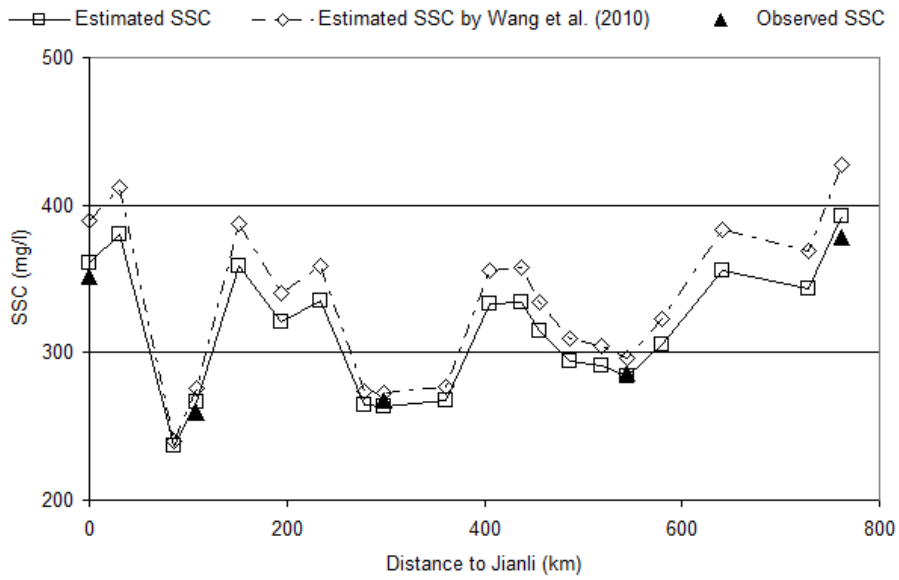

Fig. 4 Observed and estimated SSC variations with increasing distance to Jianli on 10 September 2005 along the Yangtze River from Jianli down to Datong.

from a Terra MODIS image (Fig. 4). As noted previously, the same image and the same 20 sites also were used in this study.

In Wang *et al*. (2010), the ARE values were 10.6%, 6.3%, 1.7%, 3.7%, and 13.1% at these five stations with sediment records (i.e. Jianli, Luoshan, Hankou, Jiujiang and Datong), respectively, and the mean ARE was 7.1%. In contrast, in the present study, the ARE values were 2.6%, 2.8%, 1.5%, 0.8%, and 3.9%, respectively, and the mean ARE was 2.3%. Clearly, equations (4) and (5), developed during this study, resulted in much more accurate SSC estimations than the single model developed by Wang *et al*. (2010).

Figure 4 clearly shows that the estimated SSC values generated during this study are much closer to the observed ones at the five hydrologic stations with sediment records in comparison to those generated by Wang *et al.* (2010). This is particularly true at the Jianli and Datong stations where the SSC values in Wang *et al*. (2010) displayed more marked overestimation errors. SSC estimations, based on regression models *in lieu* of actual sample data, are crucial for accurately mapping SSC spatial variations along the Middle and Lower Yangtze River. Such SSC spatial distributions can be used to investigate sediment transport and deposition in the main channel, as well as from the interactions between the mainstem and its tributaries (e.g. the Hanjiang River) and interconnected lakes, such as at Dongting and Poyang (Fu *et al*., 2003), or as the result of climate effects, or human activities such as dam construction and illegal sand extraction (Xu, 2007).

CONCLUSIONS

(1) SSC is a critical parameter in the study of river sediment transport and water quality variations; however, SSCs determined using conventional measurement methods are expensive and time-consuming.
(2) To overcome these disadvantages, remote sensing data have been applied to estimate the SSC of water bodies during past decades.
(3) Previous studies found that even for large highly turbid rivers such as the Yangtze, Landsat ETM+ and Terra MODIS images could provide a relatively accurate SSC estimate; however, it also was found that samples with elevated SSCs were systemically underestimated because water reflectance exhibited saturation behaviour with increasing SSC.
(4) The present study focused on the nonlinear relation between spectral reflectance and the SSC of turbid rivers and applied a simple segmented linear regression to directly estimate the SSC of the entire reach of the Middle and Lower Yangtze River from MODIS images.
(5) Although prior studies employed the same MODIS spectral data, the same SSC data, and the same study sites, this study largely improved the accuracy of SSC estimations, particularly for sites/samples with high SSC values.
(6) This is crucial for studying SSC spatial and temporal variations in large rivers as they reflect changes in climate and various anthropogenic activities such as dam construction and illegal sand extraction.
(7) The regression relationship developed in this paper may change from year-to-year, and this potential problem will be considered in future work.

Acknowledgements This research was supported by the University of New Brunswick Canada Research Chairs Program. J. J. Wang is the winner of the World Future Foundation PhD Prize in Environmental and Sustainability Research for the AY2010/2011.

REFERENCES

Bowers, D. G., Boudjelas, S. & Harker, G. E. L. (1998) The distribution of fine suspended sediments in the surface waters of the Irish Sea and its relation to tidal stirring. *Int. J. Remote Sens*. 19(14), 2789–2805.

Dai, Z. J., Chu, A., Stive, M, Du, J. Z. & Li, J. F. (2011) Is the Three Gorges Dam the cause behind the extremely low suspended sediment discharge into the Yangtze (Changjiang) Estuary of 2006? *Hydrol. Sci. J*. 56(7), 1280–1288.

Dekker, A. G., Vos, R. J. & Peters, S. W. M. (2002) Analytical algorithms for lake water TSM estimation for retrospective analyses of TM and SPOT sensor data. *Int. J. Remote Sens*. 23, 15–35.

Doxaran, D., Froidefond, J. M., Lavender, S. & Casting, P. (2002) Spectral signature of highly turbid waters: application with SPOT data to quantify suspended particulate matter concentrations. *Remote Sens. Environ*. 81, 149–161.

Fu, R., Yu, Z. Y. & Fang, H. (2003) Variation trend of runoff and sediment load in Yangtze River. *J. Hydraulic Engng* 11, 23–29 (in Chinese).

Gao, J. & O'Leary, S. M. (1997) Estimation of suspended solids from aerial photographs in a GIS. *Int. J. Remote Sens*. 18(10), 2073–2086.

Han, L. & Rundquist, D. C. (1994) The response of both surface and underwater light field to various levels of suspended sediments: preliminary results. *Photogram. Engng & Remote Sens.* 60(12), 1463–1471.

Harrington, J. A., Schiebe, F. R. & Nix, J. F. (1992) Remote sensing of Lake Chicot, Arkansas: monitoring suspended sediments, turbidity, and secchi depth with Landsat MSS data. *Remote Sens. Environ*. 39, 15–27.

Islam, M. R., Yamaguchi, Y. & Ogawa, K. (2001) Suspended sediment in the Ganges and Brahmaputra Rivers in Bangladesh: observation from TM and AVHRR data. *Hydrol. Processes*, 15, 493–509.

Lathrop, R.G. Jr. & Lillesand, T.M. (1989) Monitoring water quality and river plume transport in Green Bay, Lake Michigan with SPOT-1 imagery. *Photogram. Engng & Remote Sens*. 55, 349–354.

Li, Q., Yu, M., Lu, G., Cai, T., Bai, X. & Xia, Z. (2011) Impacts of the Gezhouba and Three Gorges reservoirs on the sediment regime in the Yangtze River, China. *J. Hydrol.* 403(3-4), 224–233.

Long, H. L., Heilig, G. K., Wang, J., Li, X. B., Luo, M., Wu, X. Q. & Zhang, M. (2006) Land use and soil erosion in the upper reaches of the Yangtze River: some socio-economic considerations on China's Grain-for-Green Programme. *Land Degradation & Development* 17(6), 589–603.

Lu, X. X. & Higgitt, D. L. (1998) Recent changes of sediment yield in the Upper Yangtze, China. *Environ. Manage*. 22(5), 697–709.

Ma, R. & Dai, J. (2005) Investigation of chlorophyll-a and total suspended matter concentrations using Landsat ETM and field spectral measurement in Taihu Lake, China. *Int. J. Remote Sens*. 26(13), 2779–2787.

Ma, W. B, Wang, F., Zhai, Q, Yang, X., Zhou, Y. & Zhou, W. B. (2011) Study on potential ecological risk assessment of sediment from the Yangtze River (Chongqing Downtown Section) in China. *Adv. Materials Res.* 414, 262–267.

Martinez, J. M., Guyot, J. L., Cochonneau, G. & Seyler, F. (2007) Surface water quality monitoring in large rivers with MODIS data application to the amazon basin. IEEE International Geoscience and Remote Sensing Symposium, 4566–4569.

Milier, R. L. & Mckee, B. A. (2004) Using MODIS Terra 250 m imagery to map concentrations of total suspended matter in coastal waters. Remote Sens Environ, 93, 259–266.

Ministry of Water Resources of China. (1992) Code for river suspended sediment measurement (GB 50159-92). China Planning Press, Beijing.

Nilsson, C., Reidy, C. A., Dynesius, M. & Revenga, C. (2005) Fragmentation and flow regulation of the world's large river systems. *Science* 308, 405–408.

Onderka, M. & Pekarova, P. (2008) Retrieval of suspended particulate matter concentrations in the Danube River from Landsat ETM data. *Sci. Total Environ*. 397(1–3), 238–243.

Ouillon, S., Douillet, P. & Andrefouet, S. (2004) Coupling satellite data with in situ measurements and numerical modeling to study fine suspended-sediment transport: a study for the lagoon of New Caledonia. *Coral Reefs* 23, 109–122.

Stumpf, R. P. & Pennock, J. R. (1989) Calibration of a general optical equation for remote sensing of suspended sediments in a moderately turbid estuary. *J. Geophys. Res.* 94, 14363–14371.

Syvitski, J. P., Morehead, M. D., Bahr, D. B. & Mulder, T. (2000) Estimating fluvial sediment transport: the rating parameters. *Water Resour. Res.* 36, 2747–2760.

Wang, J. J., Lu, X. X., Liew, S. C. & Zhou, Y. (2009) Retrieval of suspended sediment concentrations in large turbid rivers using Landsat ETM+: an example from the Yangtze River, China. *Earth Surf. Processes Landf.* 34, 1082–1092.

Wang, J. J., Lu, X. X., Liew, S. C. & Zhou, Y. (2010) Remote sensing of suspended sediment concentrations of large rivers using multi-temporal MODIS images: an example in the Middle and Lower Yangtze River, China. *Int. J. Remote Sens.* 31(4), 1103–1111.

Xu, G. (2007) Illegal sand extraction out of control: an ecological threat on Poyang Lake. *China Economy Times* (April 25, 2007) (in Chinese).

Yang, S. L., Milliman, J. D., Li, P. & Xu, K. (2011) 50,000 dams later: Erosion of the Yangtze River and its delta. *Global and Planetary Change* 75, 14–20.

Yang, S. L., Zhang, J., Zhu, J., Smith, J. P., Dai, S. B. & Gao, A. (2005) Impact of dams on Yangtze River sediment supply to the sea and delta wetland response. *J. Geophys. Res.* 110, F03006. doi:10.1029/2004JF000271.

Yangtze River Water Resources Commission of Ministry of Water Resources of China (2006) Yangtze River Sediment Bulletin of 2005 (in Chinese).

Zhou, W., Wang, S., Zhou, Y. & Troy, A. (2006) Mapping the concentrations of total suspended matter in Lake Taihu, China, using Landsat-5 TM data. *Int. J. Remote Sens*. 27(6), 1177–1191.